INFORMATION TO USERS

Angular momentum of light and its mechanical effects on a
birefringent medium

Padmabandu, Gamaralalage Gunasiri, M.S.

The University of Arizona, 1988

ANGULAR MOMENTUM OF LIGHT AND ITS

MECHANICAL EFFECTS ON A BIREFRINGENT MEDIUM

by

Gamaralalage Gunasiri Padmabandu
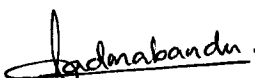
A Thesis Submitted to the Faculty of the

COMMITTEE ON OPTICAL SCIENCES

In Partial Fulfillment of the Requirements
For the Degree of

MASTERS OF SCIENCE

In the Graduate College

THE UNIVERSITY OF ARIZONA

1 9 8 8

STATEMENT BY AUTHOR

This thesis has been submitted in partal fulfillment of requriements for an advanced degree at The University of Arizona and is deposited in the University Library to be made available to borrowers under rules of the Library.

Brief quotations from this thesis are allowable without special permission, provided that accurate acknowledgment of source is made. Requests for permission for extended quotation from or reproduction of this manuscript in whole or in part may be granted by the head of the major department or the Dean of the Graduate College when in his or her judgment the proposed use of the material is in the interests of scholarship. In all other instances, however, permission must be obtained from the author.

SIGNED: _Jardanabandu._

APPROVAL BY THESIS DIRECTOR

This thesis has been approved on the date shown below:

A. S. Marathay
Professor of Optical Sciences

Dec. 12 /88 .
Date

ACKNOWLEDGMENTS

I wish to expres deep gratitude to my thesis advisor Prof. A. S. Marathay without whose valuable advice and guidance the work reported in this thesis would not have been possible. Despite his busy schedule his help was available at all times. My special thanks are due to Prof. William S. Bickel, for his enlightening discussions on the experimental aspects of the problem and for the assistance given in other possible ways.

I would like to thank Prof. S. F. Jacob, for his thoughtful support.

I am also greatful to Karen Halstead in the department of Physics, for painstakingly typing parts of the manuscript. Maggie Whitney and Mary McGoldrick in Optical Sciences whose assistance in preparing the manuscript is greatly appreciated.

Finally, I am indebted to my wife Gothami for her understanding and for her support, which can in no way be adequately expressed in words.

TABLE OF CONTENTS

LIST OF ILLUSTRATIONS

LIST OF TABLES

ABSTRACT

The torque exerted by a beam of polarized light on a half-wave plate which alters its state of polarization is calculated for several laser wavelengths and intensities using electromagnetic theory. The second-order torque that arises through the nonlinear interaction is formulated and the numerical values are calculated for the 42m crystal class. The experiment used to detect the existence of the torque is reviewed and a demonstration experiment is suggested.

CHAPTER 1

Introduction

The mechanical effects of light come from two basic properties of electromagnetic fields, namely the linear momentum carried by a beam of electromagnetic waves and the angular momentum carried by a circularly polarized beam of light. These properties have been known since the turn of the century.[1]

Classically, Maxwell's theory of electromagnetic fields explains the linear momentum of a light beam in association with the Poynting vector and hence the concept of radiation pressure is explained as a linear momentum transfer from the light beam to the material system. Lebedev[2,3] and Nicols and Hull[4] were among the first to verify experimentally the existence of radiation pressure, and the results of their experiments were in good agreement with Maxwell's theory.

The classical concept of radiation pressure has been used in various branches of physics. These areas include basic physical phenomena in plasma,[5] atomic clouds, comet tails and the internal stability of giant stars,[6] and several other areas.

In quantum theory, the concept of radiation pressure is abandoned but the momentum transfer itself is seen as the direct mechanical effect. This is well observed in the scattering of x rays from free electrons.[7] The systems considered above are all examples of radiation pressure or forces related to the linear momentum of a light beam.

The second class of mechanical effects arise from the angular momentum of a light beam. Angular momentum of a photon or a light wave is a simple concept and has been well understood in both quantum mechanics[8] and classical electromagnetic

theory.[9] In the quantum theoretical approach, the angular momentum of individual light quanta is related to the spin of photons and the concept is used in understanding conservation laws associated with dipole selection rules for electronic transitions in atoms and molecules. In the world of particle physics the photon is regarded as a particle similar to several other fundamental particles. In this theory the angular momentum is quantized.

Classical electromagnetic theory defines the angular momentum of a light wave as associated with the helicity or the state of circular polarization of the wave. Thus in the classical picture, a light wave that propagates through a medium preserving its state of polarization also preserves its angular momentum. A change in the angular momentum of the beam accompanies a mechanical torque on the medium. This effect has been studied by several authors and experimental evidence is found related to this effect.[10]

In the experimental verification of both the radiation pressure or the linear momentum, transfer and the angular momentum transfer from a light beam were initially performed by detecting the twist of a fiber in high vacuum.[2,8] Experiments were complicated because the available light sources were incoherent and thermal and the radiometric forces could easily mask the objective of the experiment. For these reasons these effects were considered to be very small or negligible in macroscopic situations.

However, the situation changed and these fields were revived with the invention of the laser in 1960's. The laser light, because of its coherence and spectral purity, can be focused to tiny spots producing very high optical power densities. Interaction of strong laser beams with atomic beams have been studied.[11,12] The momentum transfer from an intense standing wavefield of near-resonant laser radiation has been measured and the results have been in good

agreement with theoretical predictions.[13] Recent progress in both theoretical and experimental work in the field shows the possibilities for trapping or micromanipulation of accelerating atoms. Small neutral particles may be micromanipulated as well.[14-16] The ground work has been laid for radiation pressure driven interferometers in which a light mirror is suspended to swing as a pendulum.[17]

The rising interest in the mechanical effects of light motivated the present work. With the advent of high-power lasers, some experiments may be redesigned to demonstrate the effect of field angular momentum more easily and with perhaps greater accuracy. The high intensity of laser beams also necessitates investigation of higher-order nonlinear interaction and its contribution to the mechanical effects.

In this work, numerical calculations are done for the first- and second-order torques for a few commonly used crystals and an undergraduate or demonstration experiment that can be performed with available lasers is discussed.

CHAPTER 2

Mathematical Formulation of the Torque

When a beam of light passes through a doubly refracting medium it experiences a cyclic change of the state of polarization with the distance of propagation. The change in polarization arises because of the two different velocities of the orthoganally polarized field components. The change in the state of polarization causes a change in the angular momentum of the beam, which ultimately is seen as a mechanical torque on the birefringent medium.

One way to develop an expression for the torque in an anisotropic medium is to study the change in angular momentum of a light beam first and then to relate it to the torque. Alternatively, as done here, we may calculate the torque directly by using the concept of electric dipoles or the polarization in the medium.

The electric polarization P of a medium can be written as,[18]

$$P = \epsilon_0 \chi^{(1)} \cdot E + \epsilon_0 \chi^{(2)} : EE \qquad (2.1)$$

where

χ^1 = first-order susceptibility tensor (second rank)

χ^2 = second-order susceptibility tensor (third rank) .

The first term in Eq. (2.1) is the first-order polarization and the second term is the second-order or nonlinear polarization. For centrosymmetric media, the second term does not exist. It is possible to expand the polarization P for even higher orders but only the terms that include $\chi^{(1)}$ and $\chi^{(2)}$ are pertinent to our discussion. The torque that arises from the first-order polarizations is discussed in this chapter in detail and the nonlinear part is discussed in Chapter 3.

For the polarization that is linear in the electric field, the torque experienced by a unit volume of the medium can be written as

$$\tau = P \times E = D \times E \tag{2.2}$$

where

$$D = \epsilon_0 E + P = \epsilon.E \tag{2.3}$$

is the displacement vector which is linear in the electric field, and $\epsilon =$ dielectric permitivity tensor.

It will be instructive to study an example of a doubly refracting medium whose crystal axes are taken along the X,Y, and Z directions of the laboratory coordinate system in space. The E_x, E_y components of a circularly polarized beam propagating in the Z direction are

$$E_x = E_0 \cos\left[\omega t - \frac{2\pi}{\lambda} n_x z\right] \tag{2.4}$$

$$E_y = E_0 \sin\left[\omega t - \frac{2\pi}{\lambda} n_y z\right] .$$

This state of circular polarization is incident on the crystal face at $Z = 0$ (see Fig. 2.1). We wish to compute the torque on the crystal.

The dielectric tensor in our choice of coordinates is

$$\epsilon = \begin{bmatrix} \epsilon_{11} & 0 & 0 \\ 0 & \epsilon_{22} & 0 \\ 0 & 0 & \epsilon_{33} \end{bmatrix} = \epsilon_0 \begin{bmatrix} n_x^2 & 0 & 0 \\ 0 & n_y^2 & 0 \\ 0 & 0 & n_z^2 \end{bmatrix} , \tag{2.5}$$

where n_x, n_y, and n_z are the refractive indices for light polarized along 1, 2 and 3 directions.
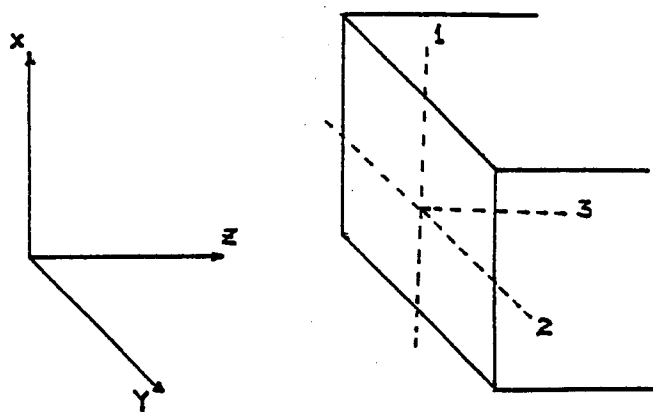
Fig. 2.1.   The system of laboratory coordinate axes and the crystal axes used in the calculation of the first-order torque.

For the special case outlined above we first compute the cross product,

$$D \times E = \frac{n_y^2 - n_x^2}{2} \epsilon_0 E_0^2 \left\{ Sin \left[2\omega t - \frac{2\pi}{\lambda} (n_x + n_y)z \right] - Sin \left[\frac{2\pi}{\lambda} (n_y - n_x)z \right] \right\}. \qquad (2.6)$$

The time averaged torque is found to be

$$\tau = \frac{1}{T} \int_0^T D \times E \, dt$$

$$= -\frac{n_y^2 - n_x^2}{2} \epsilon_0 E_0^2 Sin \frac{2\pi}{\lambda} (n_y - n_x)z \, \hat{k} \, ,$$

where $\hat{k}$ is a unit vector along Z direction. The space-averaged torque or the torque over a length Z of the crystal is found by

$$\tau(z) = -\frac{n_y^2 - n_x^2}{2} \epsilon_0 E_0^2 \int_0^z Sin \frac{2\pi}{\lambda}(n_y - n_x)z'A \, dz' \, ,$$

where A = cross sectional area of the crystal face.

After the integration we have,

$$\tau(z) = -\frac{n_y + n_x}{2\pi} \epsilon_0 E_0^2 A\lambda \, Sin^2 \frac{\pi}{\lambda} (n_y - n_x)z \, k \quad . \qquad (2.8)$$

The dependence of the torque on the initial direction of the linearly polarized incident wave has been discussed by Beth at al and is found in appendix A.

As explained in appendix A, the torque over a distance $Z_2 - Z_1$ of the crystal for initially linearly polarized light can be written as

$$\tau = \frac{n\lambda\epsilon_0 E_0^2}{\pi} \, Sin \, 2\theta \left[Sin \, \frac{2\pi}{\lambda} (n_y - n_x)z_2 - Sin \, \frac{2\pi}{\lambda} (n_y - n_x)z_1 \right] \quad . \qquad (2.9)$$

The same expression for the torque can be obtained by using the conservation of angular momentum at the faces of the crystal plate. Consider an elliptically polarized light wave propagating in the Z-direction in a vacuum. For the purpose of calculations, this could be written in different sets of basis vectors. The components of the E-vector along the principal axes of the vibration ellipse can be written, with amplitudes X_0 and Y_0, as

$$E_1^0 = X_0 \cos(\omega t - kz)$$

$$E_2^0 = Y_0 \cos\left[\omega t - kz - \frac{\pi}{2}\right]$$

Take ϵ_1, ϵ_2 to be the unit vectors along the directions of the principal axes.

The same light wave can be represented with respect to another arbitrary pair of orthogonal X and Y axes in the same plane and the components E_1 and E_2 along X and Y directions will be written as[10]

$$E_1 \equiv X\cos(\omega t - kz + \delta)$$

$$E_2 \equiv Y\cos(\omega t - kz - \delta)$$

where

X and Y are the amplitudes

2δ is the phase difference between the two components.

Now take $\epsilon_+ = \epsilon_1 + i\epsilon_2$ and $\epsilon_- = \epsilon_1 - i\epsilon_2$ as a set of basis vectors and consider the light wave as a superposition of left and right circular polarized light with amplitudes L and R respectively. Then the relationship between the field amplitudes in each representation is found[10]

$$X_0 Y_0 = XY \cdot \sin 2\delta = L^2 - R^2 \quad . \tag{2.10}$$

$$X_0^2 + Y_0^2 = X^2 + Y^2 = 2(L^2 + R^2) \quad . \tag{2.11}$$

In classical electromagnetic theory, the field angular momentum density is written as[9]

$$L_{field} = x \times g$$

$$= \frac{1}{c^2} \vec{x} \times (\vec{E} \times \vec{H}) \quad . \tag{2.12}$$

Then for a circularly polarized beam of light the time averaged component (L_3) of angular momentum parallel to the direction of propagation is found to be,

$$L_3 = \pm \frac{u}{\omega} \tag{2.13}$$

where

ω = frequency of wave

U = energy density of the wave field.

The upper sign is for the left circular polarized wave and the lower is for the right circular polarized component.

The energy per unit area per second that is carried by the left circular polarized component can be written

$$U_+ = \frac{1}{2} c\epsilon_0 L^2 \quad . \tag{2.14}$$

Using equations 2.13 and 2.14, the angular momentum carried by the left circular polarized component is found to be,

$$L_3 = \epsilon_0 \lambda L^2 \frac{}{4\pi} \quad . \tag{2.15}$$

Considering the right circular polarized component in the same way and taking the directions into account, the net angular momentum L_t transmitted per unit area per unit time is

$$L_{tot} = \frac{\lambda \epsilon_0}{4\pi} (L^2 - R^2) \equiv \frac{\lambda \epsilon_0}{4\pi} XY \sin 2\delta$$

$$\equiv \frac{\lambda \epsilon_0}{4\pi} X_0 Y_0 \quad . \tag{2.16}$$

This is the angular momentum transmitted in vacuum. To find the momentum transfer to the crystal, it is necessary to consider the reflection and refraction at the boundaries.

Assume that the birefringent medium is confined between the two planes $Z = Z_1$ and $Z = Z_2$. The X and Y components of the reflected and transmitted waves at the boundary $Z = Z_1$ can be found using Fresnel's equations and they are,

$$R_x = \frac{X(n_x - 1)}{n_x + 1}$$

$$R_y = \frac{Y(n_y - 1)}{n_y + 1}$$

$$T_x = \frac{2X}{n_x + 1}$$

$$T_y = \frac{2Y}{n_y + 1}$$

respectively.

The transmitted component, using the notation in Appendix A can be written

$$\frac{2X}{n_x + 1} = E_0 \cos\theta$$

$$\tag{2.17}$$

$$\frac{2Y}{n_y + 1} = E_0 \sin\theta$$

where E_0 is the total field amplitude in the crystal and θ is the direction of the E-vector with respect to the X-axis at the boundary $Z = Z_1$. Using the Eq. 2.16 and the

field amplitudes specified above we can calculate the net angular momentum transferred to the crystal plate at $Z = Z_1$ and it will be,

$L(z_1)$ = incident angular momentum - reflected angular momentum

$$= \frac{\lambda \epsilon_0 (n_x + n_y) XY}{2\pi (n_x + 1)(n_y + 1)} \, \text{Sin} 2\delta_1 \quad . \tag{2.18}$$

Equations 2.17 and 2.18 can be combined to yield:

$$L(z_1) \equiv \frac{\lambda \epsilon_0 \epsilon_0^{\ 2}}{2\pi} (n_y + n_x) \, \text{Sin} 2\theta \, \text{Sin} \frac{2\pi}{\lambda} (n_y - n_x) \, z_1 \quad .$$

With a similar consideration at the boundary $Z = Z_2$ and combining the Eqs. (2.17) and (2.18), the net angular momentum transmitted through the crystal plate of thickness $Z_2 - Z_1$ can be found and will be equal to

$$L(z_{2,z_1}) \equiv \frac{\lambda \epsilon_0 E_0^2}{2\pi} (n_y + n_x) \, \text{Sin} 2\theta \left[\text{Sin} \frac{2\pi}{\lambda} (n_y - n_x) z_2 - \text{Sin} \frac{2\pi}{\lambda} (n_y - n_x) z_1 \right]$$

This result is identical to the expression for the torque in Eq. (2.9). This means that the torque is equal to the excess angular momentum per unit area per second flowing in to the crystal at $z = z_1$ over that flowing out at $z = z_2$.

Quantum theory of light or the photon concept can be used to derive the same result. Each photon has an intrinsic angular momentum +h(-h) associated with its left(right) circular polarization. As a beam of light propagates through a birefringent medium, the polarization changes and the resulting change in angular momentum can be calculated simply by finding the net number of photons which change the handedness and multiplying it by the factor h. This will lead to an expression independent of h and the result will again be the same as Eq. (2.9). The calculation is straight forward and a detailed discussion is found in Ref.10.

Now we turn to discuss the Eq. 2.8, the dependence of the torque on other parameters.

$\tau(z)$ in Eq. (2.8) is plotted as a function of Z in Fig. 2.2.

The torque is a $\sin^2$ function of the thickness of the crystal plate as shown in Fig.2.2. $\tau(z)$ is a maximum when the thickness of the plate corresponds to that of a half-wave plate. It is intuitively obvious that the maximum change in angular momentum and hence the maximum torque is possible when the polarization is changed from left circular to right circular or vice versa and is achieved when a half-wave plate is used.

The magnitude of the torque can be related to the power delivered by the light wave. Assuming a uniform cross-sectioned laser beam, the power P can be written as[19]

$$P = IA,$$

where

I = the intensity of the optical field and is given by

$$I = \frac{1}{2} \text{Re}[E \times H^*]$$

and thus we have

$$P = \frac{1}{2} \text{Re } y^* E_0^2 \text{ for a medium and}$$

$$P = \frac{1}{2} \epsilon_0 c E_0^2 A \text{ for free space}$$

where

y = admittance of the medium

c = speed of light

$\tau \; (\bar{z})$

$\dfrac{A\lambda(n_y+n_x)\epsilon_0 E^2}{2\pi}$

$\dfrac{\lambda}{2(n_y-nx)}$

$\dfrac{\lambda}{n_y-nx}$

$\bar{z}$
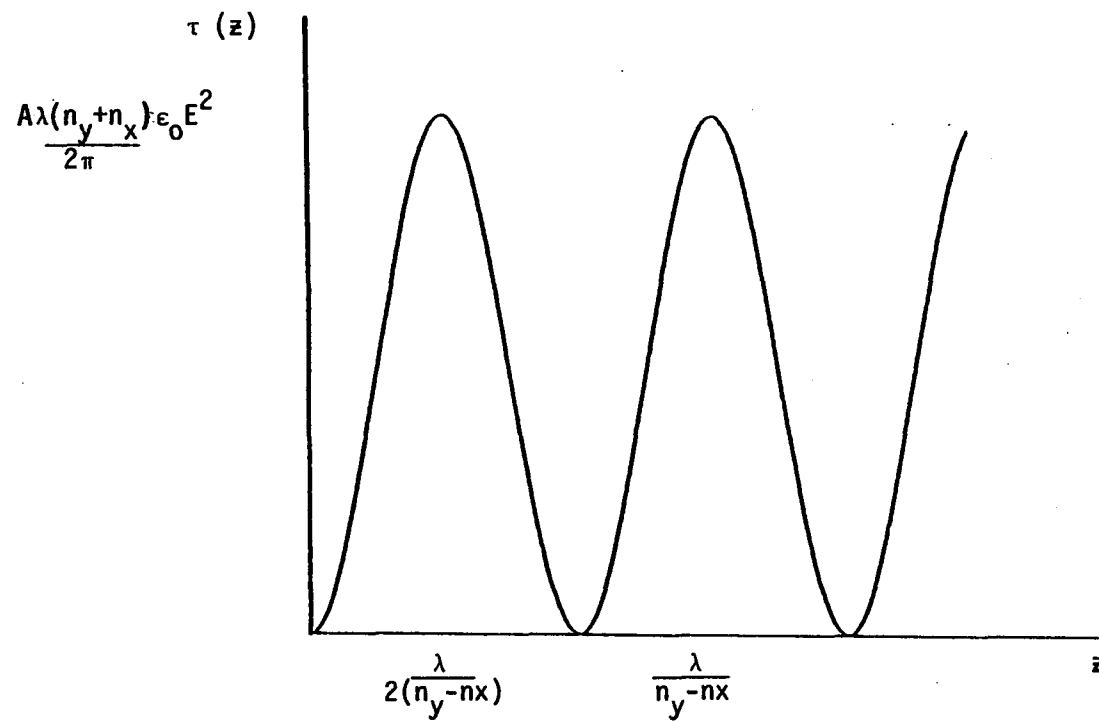
Fig. 2.2.   Variation of the first order torque with the distance
of propergation through the crystal plate.

E_0 = field amplitude

ϵ_0 = permeability of free space.

The maximum time-averaged torque for this power is written as

$$\tau_{max} = \frac{n}{\pi c} \lambda P \qquad (2.19)$$

or

$$\tau_{max} = 1.06n\lambda P \times 10^{-2} \text{ dyne c.m.} \qquad (2.20)$$

where

$n = \dfrac{n_x + n_y}{2}$ = average index of refraction in the plane perpendicular to the

direction of propagation

λ = wavelength of light in micrometers

P = power delivered by the light beam in watts.

This means that the torque experienced by the crystal plate depends only on the total power delivered to the crystal, the wavelength of the light, and the average index of the medium. Clearly, the birefringence of the medium does not affect the size of the torque, but determines the thickness of the wave plate. High-power densities are not needed. Therefore it is possible to demonstrate this effect more easily with average-power cw lasers without exciting any nonlinear interactions in the medium.

Values of the torque for several uniaxial crystals calculated using Eq. (2.20) are presented in Table 2.1. Some typical values for the laser power were used in the calculation and the direction of propagation of light was taken along the 2 axis of the crystal.

As seen from the Table 2.1, the magnitude of the torque is small and is not sufficient to induce changes in optical constants or additional birefringence in the

crystal plate. If the crystal plate is hung from a fine fiber (quartz), the torque on the crystal can twist the fiber through a very small angle. Each box in the last four columns of Table 2.1 shows the torque in dyne c.m., and the twist in degrees that can result in a quartz fiber of tortional constant 8.5×10^{-6} dyne cm rad^{-1} by the torque in the same box for commonly used uniaxial crystals.

As seen in Table 2.1, 10 W of laser can produce about half a degree rotation. Even with less power, i.e., 2 W, a rotation of a tenth of a degree is possible and is observable. As will be discussed in the Chapter 4, the rotation may be enhanced by using a series of waveplates.

Table 2.1. Calculated values for the first-order torque indifferent uniaxial crystals for several conventional laser lights.

Laser	Wave-length λ (μm)	Power (W)	Quartz	Calcite	Rutile	KDP
He-Ne	0.6328	10×10^{-3}	$\tau = 1.03\times10^{-10}$ $\theta = 6.9\times10^{-4}$	$\tau = 1.05\times10^{-10}$ $\theta = 7.07\times10^{-4}$	$\tau = 1.78\times10^{-10}$ $\theta = 1.19\times10^{-3}$	$\tau = 1.00\times10^{-10}$ $\theta = 6.74\times10^{-4}$
He-Cd	0.4412	50×10^{-3}	$\tau = 3.7\times10^{-10}$ $\theta = 2.49\times10^{-3}$	$\tau = 3.64\times10^{-10}$ $\theta = 2.45\times10^{-3}$	$\tau = 6.22\times10^{-10}$ $\theta = 4.19\times10^{-3}$	$\tau = 3.50\times10^{-10}$ $\theta = 2.35\times10^{-3}$
Ar$^+$	0.4880	10	$\tau = 8.06\times10^{-8}$ $\theta = 0.54$	$\tau = 8.20\times10^{-8}$ $\theta = 0.55$	$\tau = 1.30\times10^{-7}$ $\theta = 0.876$	$\tau = 7.75\times10^{-8}$ $\theta = 0.522$
Nd:YAG	1.06	1	$\tau = 1.33\times10^{-8}$ $\theta = 0.09$	$\tau = 1.75\times10^{-8}$ $\theta = 0.12$	$\tau = 3.01\times10^{-8}$ $\theta = 0.203$	$\tau = 1.68\times10^{-8}$ $\theta = 0.14$

τ = Torque (dyne c.m.)
θ = Rotation (degrees)

CHAPTER 3

Calculation of Higher-Order Effects

Since we found that higher powers deliver a large torque, it is also important to study the effect of crystal nonlinearities for the sake of completeness. In the calculations presented in Chapter 2, the electric polarization of the medium was assumed linear with the optical field amplitude, and the effect was termed a first-order effect. But, in fact, the torque calculated depended on the square of the electric field, or the total power delivered to the crystal.

The torque that can be calculated using nonlinear polarization is taken here as higher order terms. The first-higher order term arises from the nonlinear polarization to the second order in the electric field. For non-centrosymmetric materials, the nonlinear polarization can be written, using the second order electric succeptibility χ^2 as,

$$P^{nl} = \epsilon_0 \chi^{(2)}:EE \ ,$$

where

P^{nl} = nonlinear polarization

$\chi^{(2)}$ = the second order electric succeptibility tensor

E = optical field.

In components that can be written as[18,20]

$$P_i^{nl} = \epsilon_0 \chi_{ijk}^{(2)} E_j E_k \qquad (3.2)$$

where the indices run from 1,2,3.

The second-order contribution to the torque on a unit volume of the material can (using $\tau = P \times E$ as in the previous chapter) be written as,

$$\tau^{n\ell} = P^{n\ell} \times E$$

or

$$\tau^{n\ell} = \epsilon_{\ell mn} P_m E_n \, , \tag{3.3}$$

where

$$\epsilon_{\ell mn} = +1 \text{ cyclic}$$

$$= -1 \text{ opposite}$$

$$= 0 \text{ otherwise}$$

and each l,m,n can take any value from 1,2,3. Equations (3.2) and (3.3) can be combined to yield

$$\tau_\ell^{n\ell} = (P^{n\ell} \times E)_\ell = \epsilon_0 \epsilon_{\ell mn} \chi_{mjk} E_j E_k E_n \, . \tag{3.4}$$

In general each $\tau_\ell^{n\ell}$ (for $\ell = 1,2,3$) will be a sum of 18 terms. For most crystal classes, not all matrix elements of the χ_{ijk} tensor are nonzero. Furthermore, the number of independent elements of the χ_{ijk} tensor depends on the symmetry properties of the particular crystal class. Table 3.1 shows the 27 elements of the χ_{ijk} tensor for all crystal classes. Interchangability of the optical fields E_j and E_k in Eq. (3.2) further reduces the complexity of the χ_{ijk}^2 tensor. Thus Voigt notation can be used by contracting the last two indices in χ_{ijk}, and the resulting tensor has only 18 elements instead of 27. As shown in Table 3.1, the symmetry properties of a particular crystal class further reduce the entries in the χ_{ijk} tensor. The symbols "o" and "o" represent nonzero elements and are opposite in signs. The elements connected with lines are equal in magnitude and the equality is implied by the symmetry properties of the crystal class.

Table 3.1. The χ_{ijk} tensor for biaxial, uniaxial, and optically isotropic crystal classes. [Source: Zernike, F., and Midwinter, J. E., *Applied Nonlinear Optics* (Wiley and Sons, NY, 1973).]
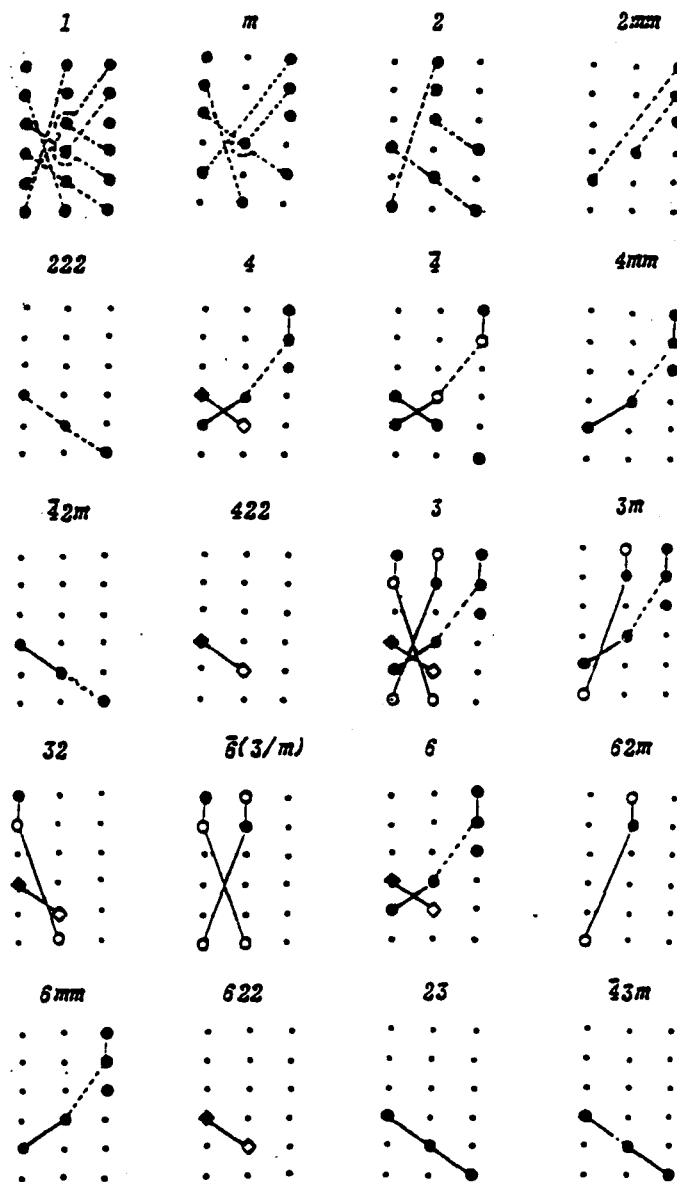
Based on Eq. (3.4) the nonlinear or the second-order torque can be calculated for all crystal classes. The size of the effect will be determined by the strength of the χ_{ijk} terms and the field amplitudes. For the work presented here we calculate and compare the nonlinear torque with the linear torque for selected crystal classes that are commonly used as nonlinear media in frequency doubling,[18] optical phase conjugation,[21] and several other applications. We show detailed calculations for one crystal class.

KDP (potassium dihydrogen phospate) and its analogues are widely used in electro-optics and in nonlinear optics. These crystals belong to the 42m crystal class. Any qualitative discussion of one of these materials applies to the group as a whole.[18] Only the numerical value of each χ_{ijk} or d_{ijk} element is different for different materials. Other useful crystals in nonliner optics are $LiNbO_3$ and $LiIO_3$, which belong to the crystal classes 3m and 6, respectively. The following section is devoted to the discussion of the nonlinear torque in the 42m crystal class.

For a given crystal class, the magnitude and the direction or the effect of the nonlinear torque depends on the direction of propagation of the wave through the crystal. Therefore the calculations are performed for two major directions of propagation, namely along and perpendicular to the optic axis.

The complexity of the calculations can be minimized by choosing the space axes to coincide with the crystal pricipal axes.

CASE 1: Wave propagation along the 3 axis of the uniaxial crystal.

Assume that the crystal 3 axis coincides with the space Z axis and takes space X and Y axes along the crystal 1 and 2 axes.

For the crystal class 42m the only nonzero elements in the χ^2_{ijk} tensor are

χ_{123} χ_{132}

χ_{231} χ_{213} ·

χ_{312} χ_{321}

If Voigt notation[18,22] is used these may be replaced by

d_{14}

d_{25}

d_{36} .

The torque calculated using Eq. (3.4) will be

$$\tau^{nl}_1 = -\epsilon_0 \ (\chi_{312} + \chi_{321})E_x E^2_y$$

$$\tau^{nl}_2 = \epsilon_0 \ (\chi_{312} + \chi_{321})E^2_x E_y$$

$$\tau^{nl}_3 = 0 \ .$$

In contrast to the first-order effect [Chapter 2] the second-order torque lies in a direction perpendicular to the direction of propagation.   Furthermore the time-averaged torque in Eq. (3.5) becomes zero unless the frequencies of the two participating field components are different.   This means that the second-order effect is possible only if two optical fields of different frequencies interact in the medium.

To investigate the problem in detail, assume two plane-polarized waves of two different frequencies are written in the form

$$E_1 = [X_1 x + Y_1 y]exp \ i(k_1 z - \omega_1 t) + c.c.$$

$$E_2 = [X_2 x + Y_2 y]exp \ i(k_2 z - \omega_2 t) + c.c. \ ,$$

where X and Y (i = 1,2) are the field amplitudes in x and y directions and x,y

are unit vectors along the crystal axes 1 and 2. Both waves E_1 and E_2 propagate along the crystal 3 axis as required for Eq. (3.5).

Substituting for Eq. (3.5), the time averaged torque is given by

$$\tau_1^{nl} = 4\epsilon_0 d_{36}\left[2Y_1 Y_2^* X_1 + Y_1^2 X_2^*\right]\exp i(2k_1-k_2)z + c.c. \tag{3.6}$$

$$\tau_2^{nl} = 4\epsilon_0 d_{36}\left[2X_1 X_2^* Y_1 + Y_2^* X_1^2\right]\exp i(2k_1-k_2)z + c.c. \tag{3.7}$$

$$\tau_3^{nl} = 0$$

for $2\omega_1 = \omega_2$ and

$$\tau_1^{nl} = 4\epsilon_0 d_{36}\left[2Y_1^* Y_2 X_2 + Y_2^2 X_1^*\right]\exp i(2k_2-k_1)z + c.c. \tag{3.8}$$

$$\tau_2^{nl} = 4\epsilon_0 d_{36}\left[2X_2 X_1^* Y_2 + Y_1^* X_2^2\right]\exp i(2k_2-k_1)z + c.c. \tag{3.9}$$

$$\tau_3^{nl} = 0 \ .$$

for $2\omega_2 = \omega_1$.

As in Chapter 2, the torque over a given length of the crystal is found by integrating over a length of the crystal.

For a plate of thickness z we get,

$$\tau_1^{nl}(z) = 4\epsilon_0 A d_{36}\left[2Y_1 Y_2 X_1 + Y_1^2 X_2\right] \cdot \frac{Sin(2k_1-k_2)z}{2k_1-k_2} \tag{3.10}$$

$$\tau_2^{nl}(z) = 4A\epsilon_0 d_{36}\left[2X_1 X_2 Y_1 + Y_2 X_1^2\right] \cdot \frac{Sin(2k_1-k_2)z}{2k_1-k_2} \tag{3.11}$$

$$\tau_3^{nl}(z) = 0$$

for $2\omega_1 = \omega_2$ and

$$\tau_1^{n\ell}(z) = 4A\epsilon_0 d_{36} \left[2Y_1 Y_2 X_2 + Y_1^2 X_1 \right] \cdot \frac{\text{Sin}(2k_2 - k_1)z}{2k_2 - k_1} \tag{3.12}$$

$$\tau_2^{n\ell}(z) = 4A\epsilon_0 d_{36} \left[2X_1 X_2 Y_2 + Y_1 X_2^2 \right] \cdot \frac{\text{Sin}(2k_2 - k_1)z}{2k_2 - k_1} \tag{3.13}$$

$$\tau_3^{n\ell}(z) = 0$$

for $2\omega_2 = \omega_1$.

As seen from Eqs. (3.10) and (3.11), for the case of $2\omega_1 = \omega_2$, the components of the torque $\tau_1^{n\ell}$ and $\tau_2^{n\ell}$ have optimum values when

$$2k_1 - k_2 = 0 \ .$$

This condition in turn demands (since $k = n\omega/c$) that

$$n_1(\omega_1) = n_2(\omega_2) \tag{3.14}$$

where $n(\omega)$ and $n(\omega)$ are the refractive indices for the electric fields polarized in 1 and 2 directions of the crystals for the respective frequencies.

For the two waves polarized in 1 and 2 directions in a uniaxial crystal, the condition $2\omega_1 = \omega_2$ and the Eq. (3.14) cannot be simultaneously satisfied. Therefore the effect is not observable in a uniaxial crystal when the direction of propergation of the two fields is along the 3 axis.

Now we turn to see the effect when the direction of propagation is perpendicular to the 3 axis of the crystal.

CASE 2 :Wave propagation along the 2 axis of the uniaxial crystal

Assume that the crystal 1,2,3 axes coincide with the x,y,z axes in the laboratory coordinate system and the two fields propagate along the y axis. The fields can have x and z components E_1 and E_2 are written as:

$$E_1 = X_1 x \exp i(k_1 y - \omega_1 t) + Z_1 z \exp i(k'_y - \omega_1 t) + \text{c.c.}$$

$$E_2 = X_2 x \exp i(k'_2 y - \omega_2 t) + Z_2 z \exp i(k_2 z - \omega_{2t}) + \text{c.c.} ,$$

where k_1 and k_1' are the wave vectors for the field components of frequency ω_1 polarized along 1 and 3 directions; k_2' and k_2 are the wave vectors for the field components of frequency ω_2 polarized along 1 and 3 directions; and they are given by

$$k_1 = \frac{\omega_1 n_1(\omega_1)}{c}$$

$$k_1' = \frac{\omega_1 n_3(\omega_1)}{c}$$

$$k_2 = \frac{\omega_2 n_3(\omega_2)}{c}$$

$$k_2' = \frac{\omega_2 n_1(\omega_2)}{c} .$$

$$(3.15)$$

With the two fields defined as above, the net field components along the x and z directions are found to be

$$E_x = X_1 \exp i(k_1 y - \omega_1 t) + X_2 \exp i(k'_2 y - \omega_2 t)$$

$$E_z = Z_1 \exp i(k'_1 y - \omega_1 t) + Z_2 \exp i(k_2 z - \omega_2 t).$$

For a plane wave propagating along the z axis, Eq. (3.5) in the previous case is modified as

$$\tau_1^{nl} = 2\epsilon_0 d_{25} E_x E_z^2$$

$$\tau_2^{nl} = 0$$

$$\tau_3^{nl} = -2\epsilon_0 d_{25} E_x^2 E_z .$$

Again we see that the component of the torque along the direction of propagation vanishes as in Eq. (3.5). For the crystal class under consideration, the torque is transverse to the direction of propagation. The time-averaged torques and

the integration over a given length of the crystal can be obtained following the same steps as in Case 1.

The time averaged torque will be

$$\tau_1^{nl} = 2\epsilon_0 d_{25} \left[Z_2^2 X_1^* \exp\, i(2k_2 - k_1)y + 2Z_2 Z_1^* X_2 \exp\, i(k_2 + k'_2 - k'_1)y + c.c. \right] \quad (3.16)$$

$$\tau_2^{nl} = 0$$

$$\tau_3^{nl} = 2\epsilon_0 d_{25} \left[2X_2 X_1^* Z_2 \exp\, i(k_2 + k'_2 - k_1)y + Z_1^* X_2^2 \exp\, i(2k'_2 - k'_1) + c.c. \right] \quad (3.17)$$

for $\omega_1 = 2\omega_2$ and,

$$\tau_1^{nl} = 2\epsilon_0 d_{25} \left[2Z_1 Z_2^* X_1 \exp\, i(k_1 + k'_1 - k_2)y + Z_1^2 X_2^* \exp\, i(2k'_1 - k'_2)y + c.c. \right] \quad (3.18)$$

$$\tau_2^{nl} = 0$$

$$\tau_3^{nl} = 2\epsilon_0 d_{25} \left[X_1^2 Z_2^* \exp\, i(2k_1 - k_2)y\ \ 2X_1 X_2^* Z_1 \exp\, i(k_1 + k'_1 - k'_2)y + c.c. \right] \quad (3.19)$$

for $\omega_2 = 2\omega_1$.

For all other frequencies which do not match the condition above, the time-averaged components of the second-order torque will vanish.

The growth of the torque with the distance of propagation is found to be

$$\tau_1^{nl}(y) = 4A\epsilon_0 d_{25} \left[Z_2^2 X_1^* \frac{\text{Sin}(2k_2 - k_1)y}{2k_2 - k_1} + 2Z_2 Z_1^* X_2 \frac{\text{Sin}(k_2 + k'_2 - k'_1)y}{k_2 + k'_2 - k'_1} \right] \quad (3.20)$$

$$\tau_2^{nl} = 0$$

$$\tau_3^{nl} = 4A\epsilon_0 d_{25} \left[X_2^2 Z_1^* \frac{\text{Sin}(2k'_2 - k'_1)y}{2k'_2 - k'_1} + 2X_2 X_1^* Z_2 \frac{\text{Sin}(k_2 + k'_2 - k_1)y}{k_2 + k'_2 - k_1} \right] \quad (3.21)$$

for $\omega_1 = 2\omega_2$ and,

$$\tau_1^{nl}(y) = 4A\epsilon_0 d_{2S}\left[2Z_1 Z_2^* X_1 \ \frac{Sin(k_1+k'_1-k_2)y}{k_1+k'_1-k_2} + z_1^2 X_2^* \ \frac{Sin(2k'_1-k'_2)y}{2k'_1-k_2}\right] \qquad (3.22)$$

$$\tau_2^{nl} = 0$$

$$\tau_3^{nl} = 4A\epsilon_0 d_{2S}\left[X_2^* Z_1^2 \ \frac{Sin(2k'_1-k'_2)y}{2k'_1-k'_2} + 2Z_1 Z_2^* X_1 \ \frac{Sin(k_1+k'_1-k_2)y}{k_1+k'_1-k_2}\right] \qquad (3.23)$$

for $\omega_2 = 2\omega_1$.

The significance of each term in Eqs. (3.20) through (3.23) depends on the relationship between the wave vectors of the two fields.

Let's define the argument (Δk_i) of the sine functions in Eqs. (3.20) through (3.23) as the phase mismatch. Then we have

$$\Delta k_1 = 2k_2 - k_1$$

$$\Delta k_2 = k_2 + k'_2 - k'_1$$

$$\Delta k_3 = 2k'_2 - k'_1$$

$$\Delta k_4 = k_2 + k'_2 + k_1$$

$$\Delta k_5 = k_1 + k'_1 - k_2$$

$$\Delta k_6 = 2k'_1 - k'_2 \ .$$

As seen from Eqs (3.20) to (3.23), the torque has a maximum as $\Delta k_i \rightarrow 0$ and oscillates sinusoidally for $\Delta k_i >> 0$. Only one Δk can be set to zero for a given set of wave vectors. This means that only one term in Eqs. (3.20) to (3.23) survives for a given configuration of k vectors and frequencies. Variation of the torque as a function of Δk_i is depicted in Fig. 3.1.
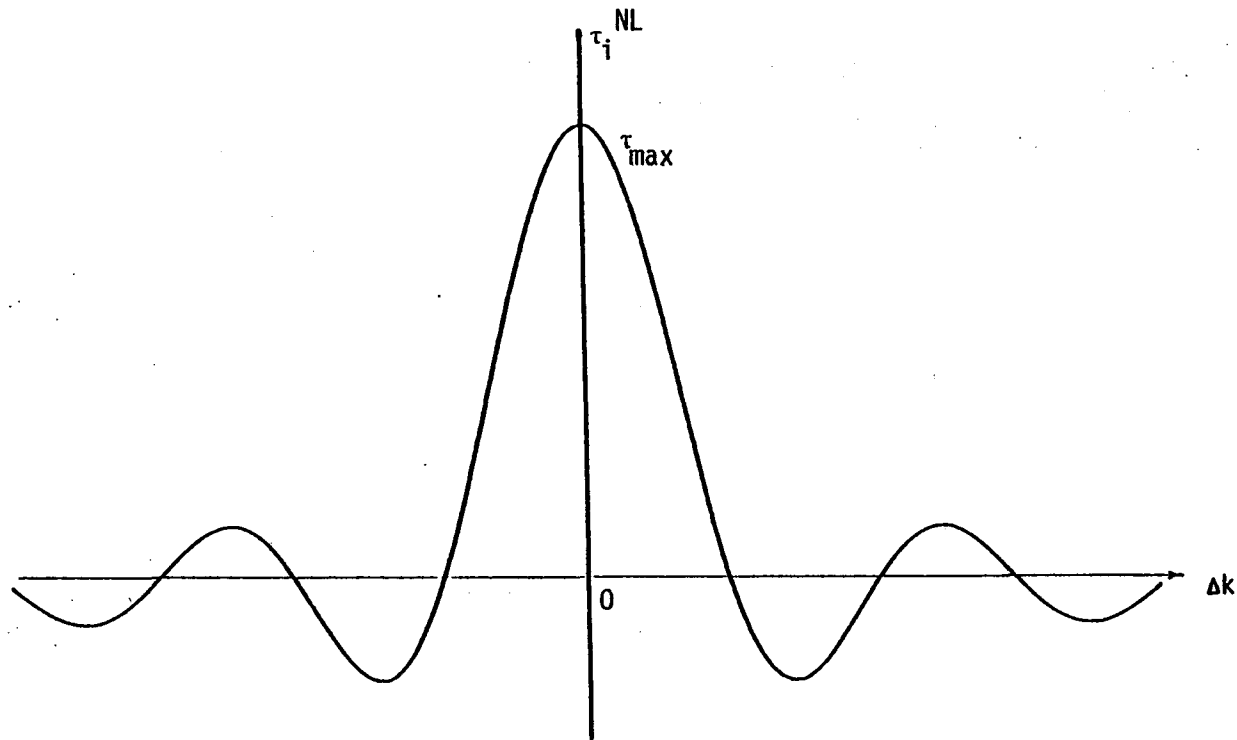
Fig. 3.1. Variation of each component of the second order torque as a function of the phase mismatch Δk. Torque has the optimum value when phase matched.

Therefore the maximum torque is obtained when properly phase matched or when $\Delta k_i = 0$. For each set of k vectors satisfying $\Delta k_i = 0$ and the frequency relationship given above, a corresponding relationship between the indices of refraction can be found using $k = n\omega/c$, and these values are given in Table 3.2.

Table 3.2. Relationships among the wave vectors, frequencies and indices of refraction to get $\Delta k = 0$ for the second-order torque.

Condition needed to give $\Delta k = 0$.	Relationship between ω_1 and ω_2.	Condition on the index of refraction.
$2K'_2 = K'_1$	$\omega_1 = 2\omega_2$	$n_1(\omega_2) = n_3(\omega_1)$
$2K'_1 = K'_2$	$\omega_2 = 2\omega_1$	$n_1(\omega_2) = n_3(\omega_1)$
$2K_1 = K_2$	$\omega_2 = 2\omega_1$	$n_3(\omega_2) = n_1(\omega_1)$
$K_1 + K'_1 = K_2$	$\omega_2 = 2\omega_1$	$n_3(\omega_2) = \dfrac{n_1(\omega_1) + n_3(\omega_1)}{2}$
$K_2 + K'_2 = K'_1$	$\omega_1 = 2\omega_2$	$n_3(\omega_1) = \dfrac{n_3(\omega_2) + n_1(\omega_1)}{2}$

The conditions found in Table 3.2 on the index of refraction are exactly the same as the conditions required for various types of second-harmonic generation in uniaxial crystals. Not all of these conditions are possible in one crystal, but one or two conditions can be met in a given crystal.

For example, the condition in the first row of Table 3.2 can be matched for negative uniaxials for two waves propagating along the z axis with the lower frequency polarized along the 3 axis. Figure 3.3 shows the variation of the index of refraction with the frequency for negative uniaxial and the index match at $\omega_1 = 2\omega_2$.

As shown in Fig. 3.2, it is possible to find ω_1 and ω_2 so that $n_1(\omega_2) = n_3(\omega_1)$ for this crystal class. This is the same condition required for Type 1 (ooe) noncritically phase-matched second-harmonic generation in negative uniaxials.

A similar analysis can be done with each row on Table 3.2. The first three rows correspond to noncritical Type 1 phase matching in uniaxial crystals while the last two correspond to noncritical Type 2 phase matching. (The conditions of Table 3.2 were derived assuming a wave propagating in crystal 2 direction, and thus the angle phase matching or critical phase matching was not involved.)

This means that one of the conditions of Table 3.2 is always matched when a uniaxial crystal is used for noncritically phase-matched second-harmonic generation. Therefore the effect should be readily observable in crystals that are used for second-harmonic generation. But the effect will be too small to cause any significant effect on the frequency mixing or the birefringence of the material. Thus, any attempt to make a measurement of the effect should be done with two powerful laser beams having orthogonal polarizations.

A sample calculation uses the following parameters:

$A = 1 \text{ mm}^2$

$\chi_{231} = \chi_{213} = 2d_{14} = 0.98 \times 10^{-12} \text{ m/V}$

$Z_3 = X_1 = 2.7 \times 10^4 \text{ V/m}$ (using a watt of laser) .

The torque τ_1 as a function of the crystal length L will be

$$\tau_1^{nl}(L) = 6.6 \times 10^{-11} L \text{ dyne cm.}$$
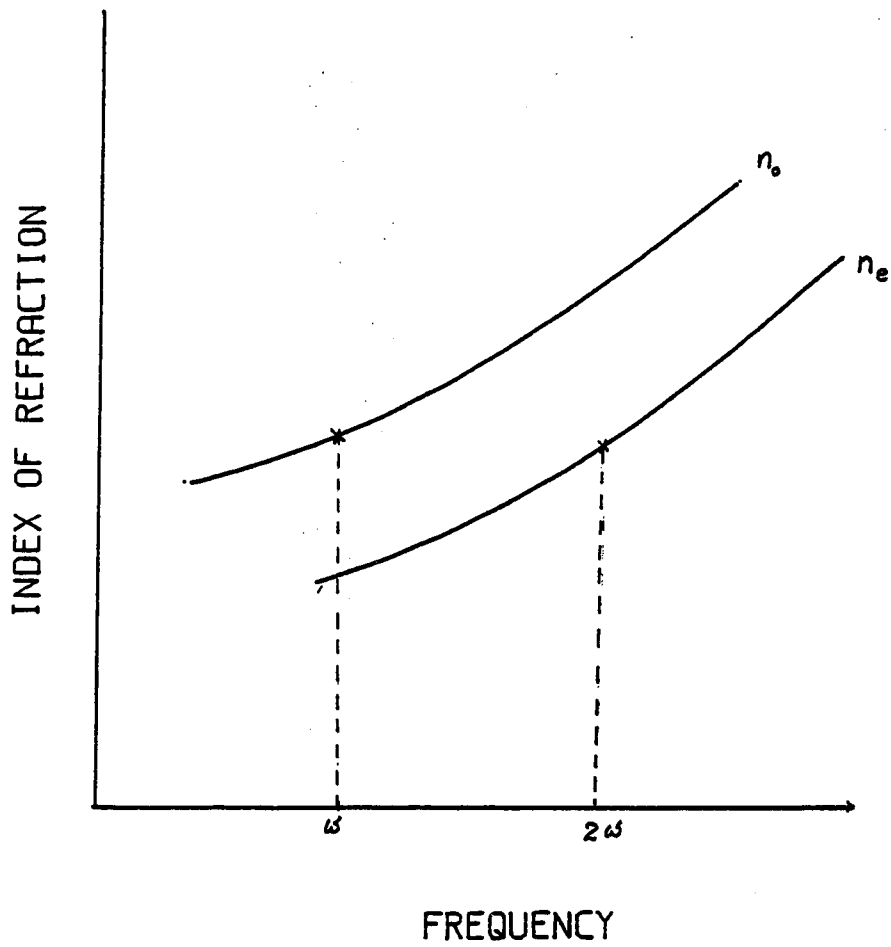
where L is in centimeters.

Fig. 3.2. Variation of the refractive index as a
function of frequency and the condition
of index matching for a negative
uniaxial crystal.

For a crystal plate of 1 cm the torque will be $\tau_1^{nl} = 6.6\times10^{-11}$ when 1 W of laser power is used. This is 1000 times smaller than the value obtained for the first-order effect.

The maximum value of the torque that can be obtained using the maximum tolerable power on the crystal is about 3.4×10^{-6} dyne cm. The power needed to create this torque is about 1.3 kW. It is not advisable to work close to the breakdown potential of materials. Since the second-order torque goes with the cube of the electric-field amplitude the reduction of the field amplitude from its maximum by a facter of 10 results in a torque of about 10^{-9} dyne cm, which is still too small to measure in the presence of other effects, e.g., the first-order torque and the radiation pressure effects.

CHAPTER 4

The Experiment

Calculations presented in previous chapters show the magnitude of torque that can be created in a waveplate using the light from a conventional laser source. The resulting mechanical stresses in the waveplate are too small to induce birefringence or changes in optical constants of the material, even with very high laser powers such as 100 MW m². Therefore, any experimental determination of the torque should be performed as a direct measurement. This is also not trivial because other mechanical or thermal disorders can easily mask the effect of such a tiny torque.

The first and the only experimental investigation on the mechanical torque was reported by Beth et al.[10] in 1935. The light source used in the experiment was a tungsten filament. The observed torque was in the range of 10^{-9} dyne cm. The experimental setup used for the detection was extremely complicated because it had been designed to eliminate or supress all possible mechanical, thermal, and electrostatic disturbances.

The purpose of the experiment was to observe torque through a rotation of a quartz waveplate hung from a fine quartz fiber. The plane of the quartz waveplate was normal to the fiber and the waveplate was illuminated normal to its surface. The torque on the waveplate created by the light beam was parallel to the fiber and the twist in the fiber was observed by measuring the deflection of a tiny beam of light that reflected from a small mirror, which had been attached to the fiber.

The waveplate and the fiber assembly was placed in a vacuum to avoid distortions from stray air currents and the fiber was surrounded by a large copper block to minimize temperature fluctuations around the fiber. Mechanical vibrations were minimized by placing the apparatus on a cast iron bracket bolted to a brick pier. As Beth et al.[10] claim, their precautions were sufficient to avoid all undesirable effects or disturbances and to measure the torque with a reasonable accuracy.

This chapter reconsiders the experiment and modifies it using new, powerful lasers that can provide a much larger torque than the light from a tungsten filament. The experiment considered here may be used as an undergraduate laboratory experiment or demonstration experiment.

Table 2.1 shows the magnitudes of the torque that can be created in a half waveplate using a conventional laser source. In the case of Ar+ and Nd:YAG lasers, the effect is fairly large and can be observed in a simple experiment. The apparatus suggested for this demonstration experiment is shown in Fig. 4.1. The catalog numbers and the manufacturer for most of the parts are found in Appendix B.

The halfwave plate hung from its center by a fine quartz fiber is placed inside a cylindrical glass chamber. The size of the chamber is not critical and can be as large as 3 in. in diameter and 7 in. high. The quartz fiber from its upper end is attached to a rotational stage that can rotate in a horizontal plane. C in Fig. 4.1 is a quarter waveplate and L is a linear polarizer. M is a plane mirror placed at 45° to the horizontal and is mounted with micro-tilt adjustments so that the light beam can be reflected in a vertical direction. The rotation of the waveplate due to the torque created by the light wave can be measured by reflecting a light beam from the tiny mirror M1, which is attached to the fiber. The scale zero can be set
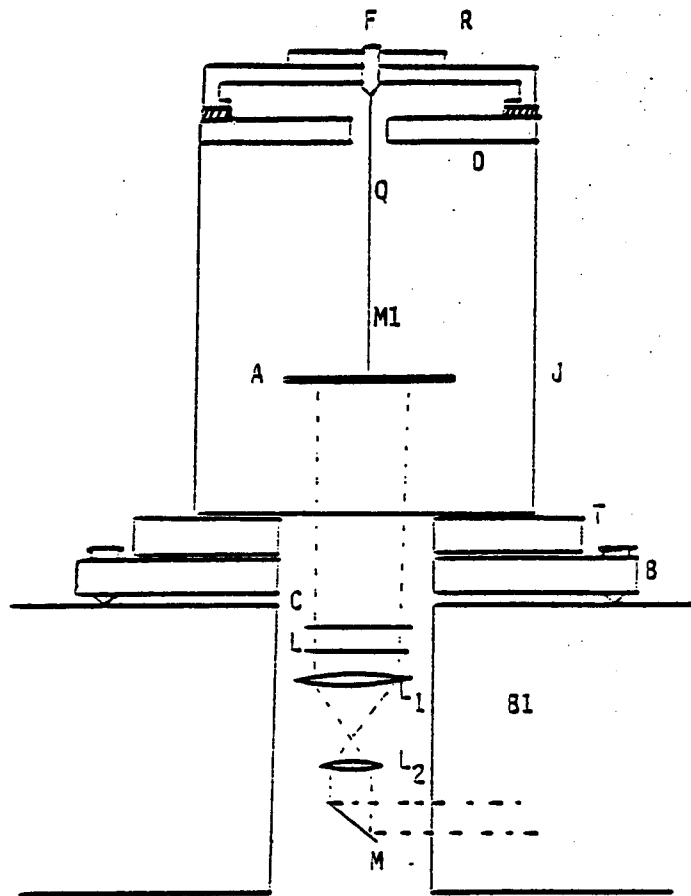
Fig. 4.1. Experimental setup for the proposed demonstration experiment. Parts are as follows:

M   = Plane mirror at 45 degrees to the horizontal.
L1,L2   = Beam expanding unit mounted with X,Y,Z adjustments.
L   = Linear polarizer
C   = λ/4 plate
S   = Beam stop to block the central part
A   = λ/2 plate
M1   = Tiny plane mirror
Q   = Quartz fiber
F   = Special fiber holder
R   = Rotational mount
D   = 1/4 inche thick copper plate
T   = X-Y translational stage
B   = metal base with 3 adjustable screws
B1   = Large metal base
J   = cylindrical glass jar.

at a desired value by turning the fiber, the mirror M1 and the waveplate arrangement, using the rotational stage described above.

T is a translational stage on which the chamber is mounted to have small translations of the chamber in the horizontal plane. These adjustments are needed to position the laser beam close to the center of the waveplate. Another alternative is to use a system of two mirror at 45^0 degrees to each other to have a universal manipulation of the laser beam. But the need of one mirror to deviate the beam from horizontal to vertical will affect the polarization properties of the beam and will reduce the efficiency of the device through a loss of intensity at reflections.

As the beam propagates through the waveplate it is necessary to have the axis of the beam as close to the fiber as possible. Not having these two centers and the center of mass of the waveplate together can cause unbalanced forces which can turn the waveplate slightly about a horizontal axis. Figure 4.2 shows the forces and torques acting on the waveplate when the forces do not have a common line of action. However, the forces from radiation pressure effects are small, since most of the light passes through the waveplate. If the waveplates specified in Appendix B are used, the force from the radiation pressure will be less than one percent of the waveplate weight. The gravitational forces can have a significant effect, depending on the weight of the waveplate. Therefore the fiber should be attached to the center of the waveplate. If this is not done, a small mass may be added to the edge of the waveplate to level.

The center of the beam should be blocked to avoid possible scattering from the fiber at the center of the waveplate. If a TEM_{00} Gaussian laser mode is used, blocking of the central part of the beam can cause large intensity losses and will reduce the overall efficiency. This problem can be reduced by expanding the laser beam and making the blocked area as small as possible. Another advantage of
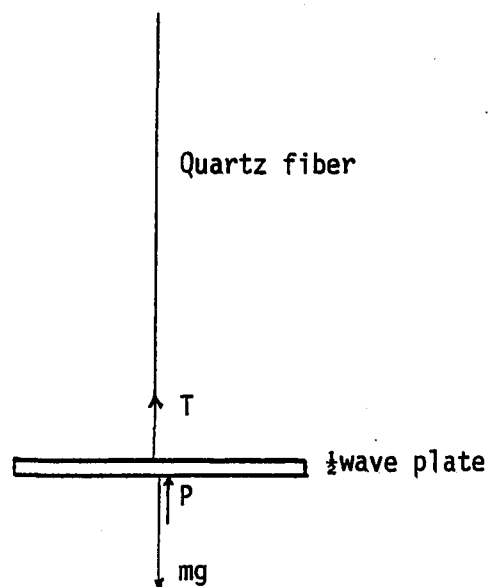
Fig. 4.2. Forces acting on the wave plate.
          T = Tension on the fiber
          mg = Weight of the wave plate
          P = Net force due to radiation pressure

increasing the beam cross section to illuminate a larger area of the waveplate is the reduction of mechanical instabilities that can arise from radiation pressure effects. If a $TEM_{01}+TEM_{10}$ or the donut mode is used, blocking the center of the ·beam will not reduce the efficiency. However, in either the $TEM_{01} + TEM_{10}$, or TEM_{00} case it is necessary to expand the beam to bring the radiation pressure effects to a minimum. This could be done by placing two microscope objectives, L1 and L2, as shown in Fig. 4.1. The power of each objective is selected based on the size of the crystal plate and the cross section of the beam from the laser source.

Polarization of the input beam is selected by rotating the quarter waveplate C and the linear polarizer L independently about the vertical axis. As discussed in Appendix A, the torque is a sine function of the angle θ between the fast axes of A and C. This can be observed by rotating the waveplate C about a vertical axis. The chamber together with the X-Y translational stage T should be mounted on a sturdy iron block with adjustable screws to avoid other mechanical disturbances.

Even though the heating effects of about 1 W of laser power are small, the effects cannot be ignored. A copper block D can be attached to the upper end of the chamber as shown in Fig. 4.1 to receive the laser power and to dissipate it as heat to the outside. In Beth's work the fiber was surrounded completely by a copper block but such precautions may not be needed when a laser is used because the torque observed is not too small.

The setup described above can be conveniently adapted for two major units as shown in Fig. 4.3a and 4.3b. One unit is the chamber with a T-translational stage and B base connected to it and the second is C,L,L1,L2, and N connected to the heavy base B1 using proper mounts. The height of the base B1 depends on the power of the microscope objectives and the size of their mounts. One of the beam-expander uints (L1,L2) needs translational adjustments along the vertical axis and in

the horizontal plane to bring the light beam to a common focus. The plane mirror M needs tilt adjustments to project the light beam in the vertical direction.

With the parts described above, we have all the adjustments necessary to accomplish the objective of the experiment.

Enhancement of the Effect

In Chapter 2 we found that the torque on the crystal plate was proportional to the change in the angular momentum of the beam. The maximum change in angular momentum is obtained when the circularly polarized light changes its handedness from one to the other and therefore the maximum torque is obtained for a single pass through a half waveplate. However there are several methods to increase the torque and hence increase the twist on the fiber.

One way to increase the torque and the twist on the fiber is to replace the copper block D by a perfect mirror to reverse both the direction and the handedness of the light beam and then send the reversed light beam through a second quarterwave plate as shown in Fig. 4.4. This was used in Beth's work,[10] which produced a torque twice as large as the torque in a single pass. The enhancement is easy to visualize when the direction of propagation and the handedness of the light beam are considered. These directions are shown in Fig. 4.4. The straight arrow shows the direction of propagation while the curved arrow shows the handedness of the light beam.

The second method is to use a series of half waveplates in an arrangement strcturally similar to a tunning capacitor of a radio circuit. This can enhance the effect to a desired degree but getting the complete mechanical alignment will be difficult.

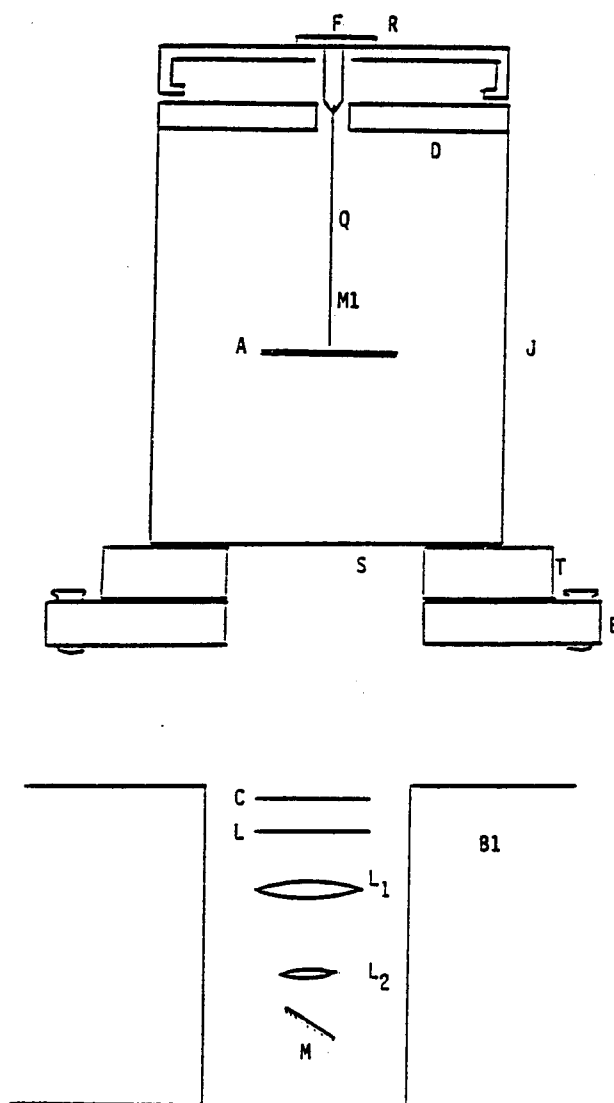Fig. 4.3. The two main units of the experimental set up. (a) The top part of the two main units of the experimental setup, and (b) beam controlling optics attached to the heavy base B1.

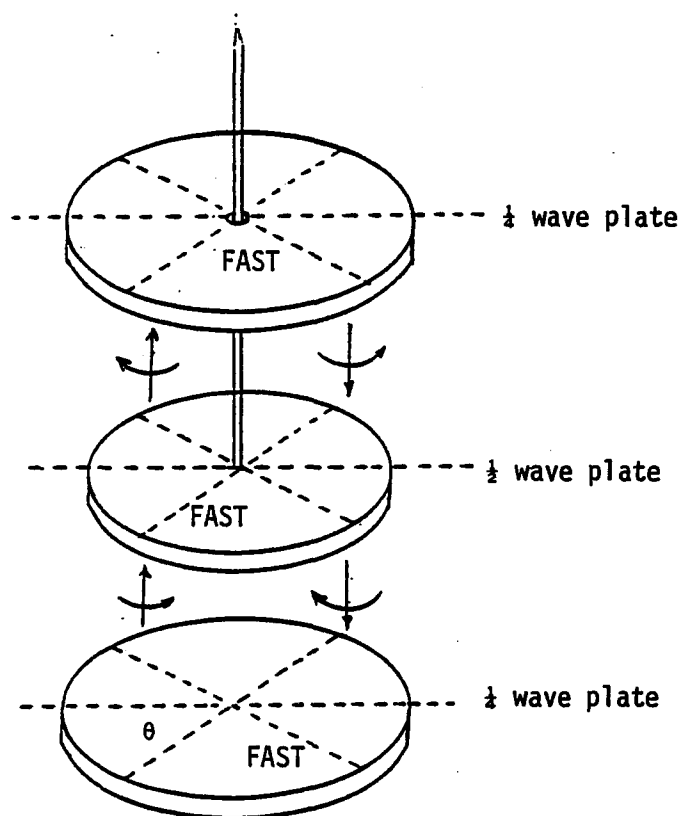Fig. 4.4. A picture very similiar to that of Beth's work showing the handedness and direction of propergation of the light when the light is reflected back after the first pass. This set-up can enhance the torque per single pass by a factor of two.

If the losses due to the reflections and absorptions at the crystal faces are neglected the weight of the stack of the waveplates and the breaking stress of the fiber will be the only limiting factors for the torsion or the observable deflection.

The arrangement consists of two sets of half waveplates. As shown in Fig. 4.5, one set of half waveplates are connected together at their centers to a unique axis which finally is connected to the fiber that suspends the whole set. The second set of half waveplates connected rigidly to the chamber with their fast axes perpendicular to those of the first set. On each fixed $\lambda/2$ plate a hole should be made at the center for the thin rod that connects the other set of waveplates.

As light propagates through the lowermost waveplate, it changes its angular momemtem and the handedness, resulting in a torque on the waveplate. Then the light passes through a fixed waveplate and regains the original handedness and this, upon transmission through the next waveplate, creates a torque in the same direction as the first. Thus, for an ideal system where absorption and reflection losses can be neglected the use of a total of N waveplates in the two sets can increase the torque by factor of $(N + 1)/2$. This means that a rotation of a tenth of a degree can be increased to one degree by arranging 19 half waveplates as above. The number of waveplates that can be used depends on the weight of the each waveplate and the breaking stress of the fiber. However, increasing the fiber diameter to support more waveplates would not produce positive results, because a 10% increment in the fiber diameter can cause about 46% reduction in the torsion or the twist. Therefore, for the best results, the maximum number of waveplates should be used with the minimum possible fiber diameter. Even though it is difficult to get the perfect alignment, the concept of stacking waveplates may produce a remarkable enhancement.
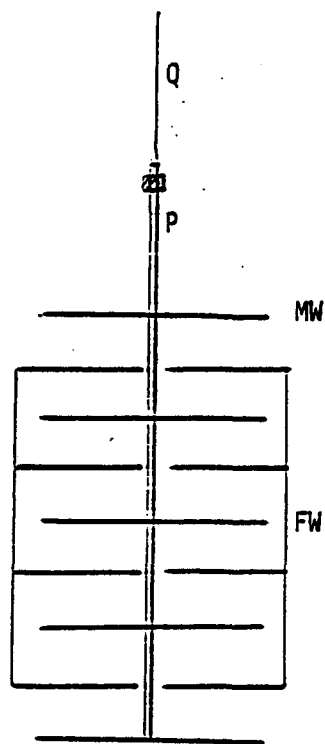
Q

P

MW

FW

Fig. 4.5. The two set arrangement of N half wave
plates which can enhance the twist on
the fiber by a factor of $\frac{N + 1}{2}$.

MW -- movable set of Wave plates.
FW -- fixed set of Wave plates.
P -- light plastic rod.
Q -- Quartz fiber.

CHAPTER 5

Conclusion

The first- and the second-order torques resulting from the change in angular momentum of polarized light in passing through a crystal plate have been calculated. The first-order torque has been measured in an earlier experiment and the results, within the limits of error, have been in agreement with theory and the work was with an ordinary tungsten filament lamp. Therefore there is no doubt that the same experiment can be done to a better accuracy with available powerful lasers.

It is also possible, as we discussed in Chapter 4, to design and build commercially the instrument to show the effect of angular momentum of a light beam or the mechanical torque exerted on a birefringent medium. This would be a great piece of equipment for undergraduate physics and optics laboratories to demonstrate a fact where the predictions from both wave and quantum theories of light come together.

As far as the second- and higher-order mechanical effects in crytals are concerned, they are still too small to be of a value in practice. Neither the first- nor the second-order mechanical effects of light in crystals and waveplates can induce strains that are large enough to cause any significant change in index of refraction or birefringence of the material. Therefore the mechanical effects in crystals seem to have a lesser importance, compared to the mechanical effects of light on very small particles.

If the current interest in the mechanical effects of light is continued, devices based on the radiation pressure and the angular momentum of light-related forces will help physicists to drive interferometers, to trap and micromanipulate small particles, and to do wonders in the years to come.

APPENDIX A

Dependence of the Torque as a Function
of the Initial Direction of the E Vector

The torque experienced by the waveplate is a function of the angle θ between the direction of initial polarization and the direction of the fast axis of the crystal face.[10]   In the derivation presented in chapter 2 this was neglected, and the calculations were done for $\theta = 45^{\circ}$.

To derive an expression for the θ dependence of the torque, assume the same coordinate system as in Chapter 2 and take the initial direction of E to be at an angle θ with the X axis. Then the field for the light wave propagated along the +Z direction is given by,

$$E_x = E_0 \; Cos\theta Cos\left[\omega t - \frac{2\pi}{\lambda} n_x \; z\right]$$

$$E_y = E_0 \; Sin\theta Cos\left[\omega t - \frac{2\pi}{\lambda} n_y \; z\right] .$$

Using the equation $\tau = D \times E$, the torque on a unit volume of the crystal is found to be

$$\tau = \epsilon_0 \; E_0^2 \left[n_x^2 - n_y^2\right] Sin2\theta Cos\left[\omega t - \frac{2\pi}{\lambda} n_x \; z\right] Cos\left[\omega t - \frac{2\pi}{\lambda} n_y \; z\right] .$$

The time-averaged torque is then found to be

$$\tau = \epsilon_0 \; E_0^2 \left[n_x^2 - n_y^2\right] Sin2\theta Cos \frac{2\pi}{\lambda} [n_y - n_x]z .$$

When averaged over the distance $Z_2 - Z_1$ of the crystal, the torque is

$$\tau(z_1,z_2) \;=\; \int_{z=z_1}^{z=z_2} \epsilon_0 E_0^2 \left[n_x^2 - n_y^2 \right] \, \text{Sin}2\theta \; \text{Cos} \; \frac{2\pi}{\lambda} \, (n_y - n_x)z \; dz$$

$$=\; \frac{n\lambda\epsilon_0 E_0^2}{\pi} \; \text{Sin}2\theta \left[\text{Sin} \; \frac{2\pi}{\lambda} \, (n_y - n_x)z_2 \; - \; \text{Sin} \; \frac{2\pi}{\lambda} \, (n_y - n_x)z_1 \right]$$

This gives the variation of the torque as a function of the distance of propagation and the angle θ between the E vector and the fast axis. For a given waveplate, the value of z is fixed and the θ dependence of the torque can be studied by changing the initial direction of the E field. Experimental details are discussed in Chapter 4. As the circular polarizer or the quarter waveplate is rotated about the vertical axis, the magnitude of the torque should trace a sine curve. This has been observed in Beth's experiment,[10] confirming the agreement with the theoretical calculations.

APPENDIX B

Suggested parts for the experiment, their catalog numbers,
specifications and the manufacturer.

Label on Fig. 4.1.	Name	Parameters	Manufacturer and the: catalog number
A	½ wave plate	thickness -- 0.75mm aperture = 15 mm material -- quartz weight - 0.8 gm thickness - 1.0 mm aperture -- 15 mm material - quartz weight -- 1.06 gm	ORIEL 25660 for λ = 514.5 nm 25639 for λ = 1.064 nm CVI Lasers QWPM - 51 - 10 - 2 for λ = 514.5 nm
C	Quarter wave plate		ORIEL 25610 for λ = 514.5 nm 25689 for λ = 1.064 nm
Q	Quartz fiber	Radius < 2 m Length - 15 cm	Should be made in a gas-oxygen flame or may be custom-made.
T	Transistional stage	1" travel 125 lb. load capacity	ORIEL 16141 New port 425A-1
J	Clear glass jar -- cylindrical	Diameter = 8 cm Height - 20 cm	
M	Mirror and the mount	Highly reflective at 45° at the laser wave length.	Mount -- Newport MM 1
L_1, L_2	Beam expanding unit (two microscopic objectives mounted with x,y,z transactional freedom)	Ratio of the powers of the two objectives depends on the input and output beam cross sections.	
B1	Solid metal base	Height = 20 cm Cross section = 8 x 15 cm	
R	Rotational mount	360° rotation	New port RSA-1
F	Fiber holder and positioner	Miniature design, versatile with x,y,z and θ, Q adjustments	New port FP-2

REFERENCES

1. J. H. Poynting, Proc. Roy. Soc. A 82, 560 (1909).

2. P. Lebedev, Ann. Phys. 6, 433 (1901).

3. P. Lebedev, Astrophysics J 31, 385 (1910).

4. E. F.Nichols and G. F. Hull, Phys. Rev. 13, 307 (1901): 17, 26 (1903).

5. C. L.Longmire, *Elementry Plasma Physics* (Interscience Publishers, New York, 1963).

6. W. G. V. Rosser, *An Introduction to Statistical Physics* (Ellis Horwood Ltd., New York, 1982).

7. R. T. Weidner and R. L.Sells, *Elementry Modern Physics* (Allyn and Bacon Inc., New York, 1980).

8. C. Cohen Tannoudji and B. Diu, *Quantum Mechanics* (John Wiley and Sons, New York, 1977).

9. J. D. Jackson, *Classical Electrodynamics, 2nd Edition* (John Wiley and Sons, New York, 1975).

10. R. A. Beth, Phys. Rev. 50, 115 (1936); 48, 471 (1935).

11. A. Ashkin, Phys. Rev. Lett. 24, 156 (1970).

12. V. A. Grinchuck, A. P. Kazantsev, E. F. Kuzin, M. L. Nagaeva, G. A. Rabeyanco, G. I. Surdutovich, and V. P. Yakovlev, Sov. Phys. JETP 59, 56 (1984).

13. P. E. Moskowitz, P. L.Gould, and D. E. Pritchard, J. Opt. Soc. Am B 2, 1784 (1985).

14. A. Ashkin, Phys. Rev. Lett. 40, 729 (1978).

15. J. Dalibard, S. Reynaud, and C. Cohen-Tannoudji, J. Phys. B 17, 4577 (1984).

16. W. D. Phillips, ed. *Progress in Quantum Electronics* (Pergamon, New York, 1984), p. 115.

17. P. Meystre, E. M. Wright, J. D. McCullen, and E. Vignes, J. Opt. Soc. Am. B 2, 130 (1985).

18. F. A. Hopf and G. I. Stegeman, *Applied Classical Electrodynamics, Vol. 2 Nonlinear Optics* (John Wiley and Sons, New York, 1985).

19. R. K. Wangsness, *Electromagnetic Fields, 2nd Edition* (John Wiley and Sons, New York, 1986).

20. Y. R. Shen, *The Principles of Nonlinear Optics* (John Wiley and Sons, New York, 1984).

21. A. Yariv, *Optical Electronics 3rd Edition* (Holt, Rinehart and Winston, New York, 1985).

22. T. Tamir, ed. *Topics in Applied Physics, Vol.7, Integrated Optics* (Springer-Verlag, New York, 1985).